Microalloying with Vanadium for Improved Cold Rolled TRIP Steels

C. Scott, F. Perrard, P. Barges

Automotive Research Center, Arcelor Research S.A.
Voie Romaine
57283 Maizières-lès-Metz
Tel:00(33).3.87.70.47.82
Fax:00(33).3.87.70.47.12
E-mail:colin.scott@arcelor.com

Abstract : Flat carbon steel manufacturers are currently developing new Transformation Induced Plasticity (TRIP) steels as a response to strong demands for vehicle lightening and security reinforcement from the automobile sector [1] . These advanced grades exhibit a very favourable compromise between strength and ductility compared to conventional steels and can therefore be produced in lighter, thinner gauge strips with equivalent functional properties. The excellent mechanical properties of TRIP steels are attributed to the high strain hardening coefficient generated by the progressive transformation of metastable retained austenite to martensite during plastic deformation. In this paper we will discuss the improvements in cold strip properties that can be obtained using vanadium microalloying in these steels. By choosing an appropriate composition and thermomechanical process path, a high fraction of the added vanadium can be made to precipitate in ferrite during the continuous annealing step, providing a large strengthening effect. This gain in strength is obtained without any significant loss of ductility as, apart from a useful grain refining effect, the presence of vanadium does not significantly modify the original TRIP microstructure.

1 Introduction

The exceptional mechanical properties of TRIP steels are due to their multiphase structure: a soft ferrite matrix with a strong bainitic phase and a suitable proportion of retained austenite. The retained austenite is stabilised during coiling for hot rolled TRIP steels or during the over ageing step for cold rolled TRIP steels. This phase is crucial because austenite stability determines the final mechanical properties. The main parameters that determine austenite stability at room temperature are the carbon content (0.5%～1.8%) and the austenite island size and morphology [2,3] . Commercial TRIP steels with ultimate tensile strengths of up to 800MPa are generally based on carbon-manganese-silicon steels with a typical composition Fe-0.2C-1.5Mn-1.5Si. Recently, low Si TRIP steels using Al and P have been developed, principally to reduce the galvanising problems encountered with high Si contents[4]. However, Al based TRIP solutions show reduced tensile properties as Al does not possess the same solid solution strengthening effect as Si. The demand for the highest strength TRIP grades (1000～1200MPa) for automobile applications can be met by increasing the carbon concentration to around 0.4%, however these higher carbon levels introduce serious weldability problems and may cause hot rolling difficulties particularly for wide formats. Precipitation hardening by microalloying additions (Ti, Nb, V) is an interesting alternative to increasing the carbon concentration and has the major advantage that weldability and hot rolling parameters are not degraded.

1.1 Definition of the microalloying composition

Several studies have shown that microalloyed TRIP steels with Nb and/or Ti can give good mechanical properties, but with a rather poor robustness [2,4~7,10]. However, very few studies exist on vanadium additions [8,9]. The ideal microalloying element for cold rolled and annealed TRIP steels should have the following properties:

(1) Large precipitates formed in slabs can be redissolved during reheating.

(2) No significant increase in hardness during hot rolling and no decrease in hot ductility.

(3) No precipitation during finishing and coiling (to facilitate cold rolling).

(4) Intense precipitation during continuous annealing.

(5) Precipitation should occur as far as possible only in the ferrite phase.

(6) Precipitation should be intragranular.

(7) The number density of precipitates should be as high as possible.

(8) Precipitates should not reduce the stability or volume fraction of retained austenite.

Points 1, 2, 3 and 5 require that the precipitating species should be highly soluble in austenite. Points 4, 6 and 7 require the maximum possible precipitation driving force to generate a high particle nucleation density. Concerning point 6, intragranular precipitation will dominate if the precipitation step occurs in a deformed matrix i.e. during annealing after cold rolling. Finally, point 8 would seem to favour the precipitation of nitrides or carbonitrides rather than pure carbides, which would tend to reduce the amount of carbon available to stabilise the residual austenite during the bainitic transformation. Taking into account all of the above criteria, the microalloying element which best satisfies these constraints is vanadium.

1.2 Precipitation of vanadium

The equilibrium solubility products for microalloy carbides and nitrides in austenite show that VN is the nitride which has the greatest solubility in austenite and that VC is even more soluble in austenite and in ferrite [11]. For the purposes of precipitation strengthening in TRIP grades, it is the precipitates formed in ferrite that are the most effective. Our objective therefore is to maintain the V in solution in the hot coil and to precipitate during continuous annealing after cold rolling. Due to the short holding times available in commercial continuous annealing lines (<200s) we need to add the correct amount of nitrogen to accelerate the nucleation step but not so much that there is significant VN precipitation in the hot coil1. Lagneborg et al. [12] have calculated the chemical driving force for VC and VN precipitation as a function of vanadium and nitrogen contents (0.06%＜V＜0.15%, 0.005%＜N＜0.015%) in steels with a carbon concentration of 0.1%. They found that increasing the nitrogen concentration was an important factor in boosting the precipitation driving force in ferrite, in agreement with the work of Ballinger and Honeycombe [13].

2 Experiments and Modelling

From the preceding discussion, it is evident that microalloying with vanadium is potentially compatible with the criteria defined in §1.1. The following sections discuss the laboratory simulations and modelling carried out in order to determine the influence of vanadium precipitation on TRIP metallurgy and mechanical properties.

2.1 Experimental laboratory casts

Table 1 shows the composition of three 15 kg laboratory casts studied in this work. The concentrations are all given in %wt. Cast A is a standard TRIP 800 composition while casts B, and C contain increasing concentrations of V and N. As regards the precipitation of VN, all

1. At equilibrium, some vanadium will precipitate in austenite especially in the presence of nitrogen, however, the kinetics of V(C,N) formation in austenite are slow and, given the fast cooling and low coiling temperatures available in TRIP

of these grades are strongly over stoechiometric in V (by a factor of between 2.5 and 5).

Table 1 Composition of laboratory heats expresses in %wt.

Laboratory Heat	C	Si	Mn	Ti	V	N
A	0.197	1.475	1.510	0.0021	0.0035	0.0016
B	0.186	1.477	1.528	0.0024	0.1081	0.0081
C	0.189	1.472	1.527	0.0026	0.2145	0.0157

2.1 Calculation of the precipitated fractions at equilibrium

It is possible to calculate the volume fraction of V, C and N which should be precipitated at equilibrium in austenite. Figure 1 is an equilibrium calculation of V(C,N) precipitation for cast C using the Arcelor CEQSCI software [15] .The solubility products used for VC and VN in austenite were from the literature [11] (concentrations in %wt):

VN (γ) : log10Ks=－7840/T+ 3.02

VC (γ) : log10Ks =－9500/T + 6.72

It can be seen that the vanadium precipitation start temperature is 1180℃. Above 1100℃ the precipitates are essentially pure nitrides. Below this temperature, the carbon content in the precipitates increases until at around 920℃ nearly all of the available nitrogen has precipitated. Below 920℃carbon either precipitates as pure VC or increases the carbon content in pre-existing V(C,N). At equilibrium, the vanadium is completely precipitated at 700 ℃. These calculations suggest that all of the available nitrogen and most of the vanadium is precipitated in the austenitic region i.e. during hot rolling. This is not at all the desired scenario for precipitation strengthening. However, these are equilibrium calculations where kinetic effects are not taken into account.

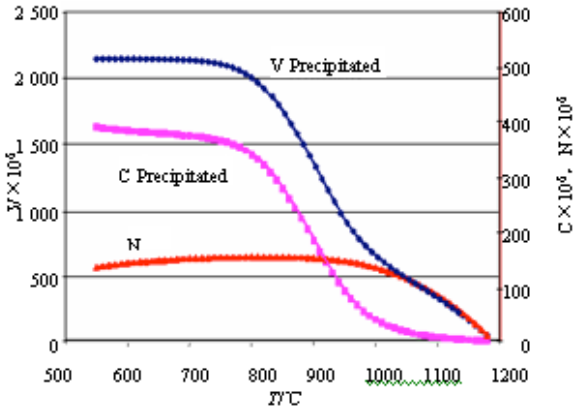

Fig.1 Equilibrium calculation of V(C,N) precipitation using the CEQSCI software for laboratory heat C (Fe-0.2C-1.5Mn-1.5Si-0.22V-0.015N)

2.2 Hot rolling simulation

The hot rolling parameters were chosen in order to minimise V precipitation in the hot strip, both for ease of cold rolling and to maximise the potential for strengthening in the cold strip.

- Reheating at 1200℃ for 15 minutes in an argon atmosphere.
- Reduction from approximately 20mm to a final thickness of 4mm.
- End rolling temperature above Ar_3 (＞900℃).
- Either water quench to ambient or fast water cool to coiling temperature (540℃).

Table 2 Mechanical properties of hot strips after coiling at 540 ℃

HEAT	YS /MPa	UTS/MPa	TEl/%	UEl/%	YPEl/%
A (Reference)	510	703	21.9	12.9	1.5
B	679	832	14	9.8	1.2
C	740	917	12.5	7.9	0.0

After coiling at 540℃, the microstructure was mixed ferrite/bainite/pearlite in all cases. The mechanical properties were measured in the transverse direction using ISO 12.5mm×50mm tensile test specimens. Table 2 gives the results for heats A, B and C.

It is interesting to note that $\Delta UTS_{(B-A)}$= +129MPa and ΔUTS(C-A) = +214MPa after coiling. These figures are very close to those estimated from Vickers' hardness

measurements of the same three heats in the as-cast condition (+141MPa and +219MPa respectively). At first inspection, this suggests that in the hot strip the added hardening component due to microalloying with V is not sensitive to the cooling rate.

2.3 Cold rolling and continuous annealing (CA) simulations

The hot strips from heats A and B were mechanically reduced to a thickness of 2.8mm and then cold rolled in 7 passes to 0.7mm (75% reduction). The hot strip from heat C was cold rolled directly from 3.92mm to 1mm in 11 passes (74.5% reduction). The type of annealing cycle simulated is shown in Figure 2. Three different intercritical annealing temperatures were tested (770℃, 790℃ and 810℃). A single overaging temperature of 400℃ was tested for heats A and C. For heat B, three different overaging temperatures, 375℃, 400℃ and 425℃ were tested. The mechanical properties were measured in the transverse directions using ISO 12.5mm×50mm tensile test specimens.

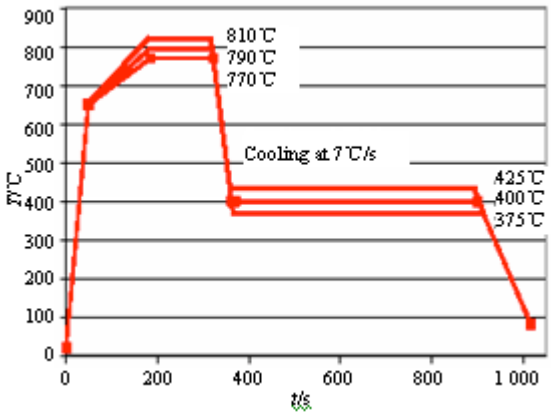

Fig.2 Simulated continuous annealing cycles.

The resulting mechanical properties are shown in figure 3. The first point of interest is that the reference composition heat A has an ultimate tensile strength of 720MPa. This is considerably lower than the expected level of 800MPa, however the total elongation is good (30%) and the product UTS*TEL is high (～21000% MPa).

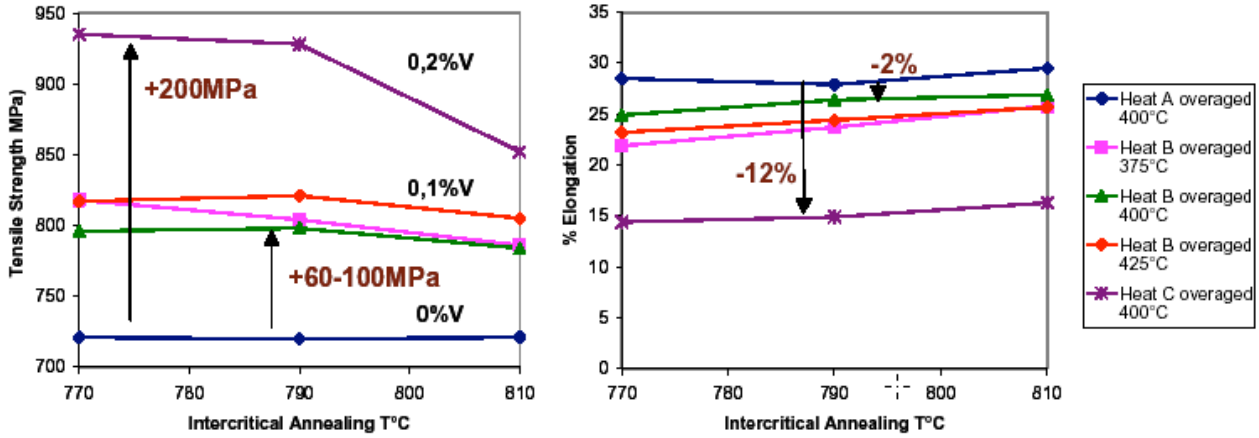

Fig.3 Tensile strength and total elongation of laboratory heats as a function of intercritical annealing and overaging temperatures

The mechanical properties of the reference heat A are not strongly modified by intercritical annealing temperatures between 770℃ and 810℃ and the highest ductility is achieved at the highest annealing temperature. The effect of microalloying on the mechanical properties is immediately obvious. In the case of heat B, compared to the non-microalloyed state, microalloying with 0.1V+0.007N gives +60~100MPa strengthening while maintaining good total elongation (TEl = 25%-27% with overaging at 400℃). For heat C, the increase in strength is much greater (up to +214MPa), however this strength improvement is achieved

at the expense of a drastic reduction in ductility (TEl = 16%). The microalloyed heats are more sensitive to the intercritical annealing temperature, especially heat C; tensile strength decreases and ductility improves as the annealing temperature increases. The next sections attempt to explain these observations by quantitative analysis of the microstructure and by modelling. We will concentrate mainly on heats A and B with intercritical annealing at 790℃ and overaging at 400℃.

2.5 Quantitative microstructural analysis of cold strips

Four phases were detected in the final microstructure; ferrite, bainite, residual austenite and a small amount of pearlite. The phase fraction and average grain size of the ferrite was determined by image analysis. The fraction of residual austenite was obtained from image analysis and from X-ray diffraction. This data is summarised in Table 3. The following conclusions are drawn:

- The presence of vanadium does not significantly modify the final ferrite fraction in the cold strip.
- The presence of vanadium does appear to refine the final ferrite grain size.
- The phase fraction of retained austenite is very similar in both cases.
- The carbon concentration in retained austenite measured by XRD was identical.
- A small amount of pearlite was detected in both cases.

Table 3. Summary of the microstructure data for heats A and C after annealing at 790°C and overaging at 400°C

Phase	Heat A	Heat B	Method
Intercritical ferrite	52 ± 5%	55 ± 5%	Image analysis
Ferrite grain size	3.2 ± 0.2μm	2.4 ± 0.2μm	Intercept method
Residual austenite	9.4 ± 1.5%	9.9 ± 1.5%	Image analysis
	7.8 ± 0.4%	8.4 ± 0.6%	XRD
% C in residual austenite	1.2%	1.2%	XRD
Bainite + pearlite	39%	36%	Estimated

These observations help to explain some of the mechanical properties data presented in Figure 3. Firstly, the presence of pearlite in the cold strip indicates that the cooling rate of 7℃/s is too slow. The quantity of residual austenite formed is thus lower than in a standard TRIP800 steel (this is typically 13%～14% for an industrial grade with a similar composition to heat A) which explains the low UTS of 720MPa in the non-microalloyed grade. An important point to note is that microalloying does not seem to affect the concentration of carbon, and hence the stability, of the retained austenite. In conclusion, the microstructure of heat B is practically identical to that of heat A except for a refinement in the ferrite grain size. A calculation carried out using the latest structure/properties model for TRIP steels developed at Arcelor [16] shows that this difference is not enough to account for the 80MPa difference in UTS, which must therefore be attributed to precipitation strengthening.

2.6 Evolution of the precipitated fractions of V and N

The amount of V and N precipitated at various stages in the fabrication process was measured using selective dissolution and chemical analysis and the results are shown in figure 4. The first remark to make concerns the precipitation of vanadium in the ingots. It is

clear that, in contradiction to the predictions of the equilibrium calculation shown in figure 1, even under slow ingot cooling a large fraction of the total vanadium is not precipitated. For cast B, only 55% of the total available vanadium is precipitated. In contrast, the measured fraction of vanadium precipitated in cast C is found to be 77%. We attribute this increase in the precipitated fraction of vanadium to the higher level of nitrogen present in this cast. Regarding the fraction of the available vanadium precipitated in the hot strips quenched from 900°C, the figures for casts B and C are 3% and 7% respectively.

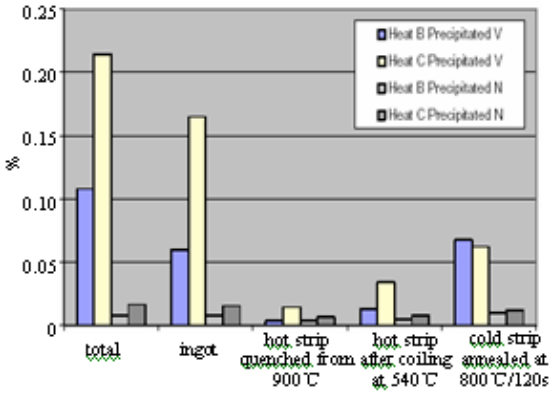

Fig.4 Evolution of the precipitation of V and Nat different stages in the simulated process.

These figures are very much less than the value of 63% precipitated fraction of vanadium predicted by the equilibrium calculation of figure 1. Thus it can be expected that, under an isothermal industrial conditions, most of the vanadium will be free to precipitate in ferrite. The increase in the fraction of V and N precipitated after continuous annealing is due either to coarsening of existing hot strip precipitates or a further nucleation step or a combination of the two. This will be discussed in detail in the next section.

2.7 Precipitation in the hot and cold bands

Substoichiometric alumina TEM extraction replicas developed at Arcelor [17] were employed to determine the size histograms of precipitates in hot and cold strips from heat B. An advantage of these alumina replicas is that they contain no carbon, so that quantitative measurements of C and N concentrations could be carried out using parallel electron energy loss spectroscopy (PEELS). The concentrations of V and Ti were determined by EDX. All TEM specimens were examined in a liquid nitrogen cold stage (-170°C) in order to eliminate the effects of carbon pollution. The analysis conditions are described elsewhere [18] .

Figure 5a shows the ferrite / bainite / pearlite microstructure of the heat B hot strip after coiling. Large cementite precipitates are extracted from the bainitic and pearlitic regions. The cold strip microstructure can be seen in the replica of figure 5b, which shows evidence of inhomogeneous distribution of precipitation in the different phases present. There appears to be a much more intense precipitation present in the cold strip ferrite than in the residual austenite or bainitic ferrite. This will be discussed further in §2.9. The V precipitate size distributions in the hot coiled state and in the cold rolled and annealedstate were determined, based on measurements of 400 precipitates for the hot coiled specimen and 535 precipitates for the cold rolled specimen. The smallest precipitates measured were 1.4 nm in radius and the largest 25 nm. Figure 6 shows the clear difference between the two specimens. The average precipitate radius decreases from 7.5 nm in the hot coil to 5.8nm in the cold strip. Bearing in mind the fact that chemical extraction experiments show that the fraction of V precipitated strongly increases in the annealing stage, the decrease in the mean precipitate radius shown in figure 6 can only be interpreted as being due to the formation of new precipitates (rather than due to the partial dissolution of existing precipitates). We conclude that a fresh precipitation step occurs during continuous annealing.

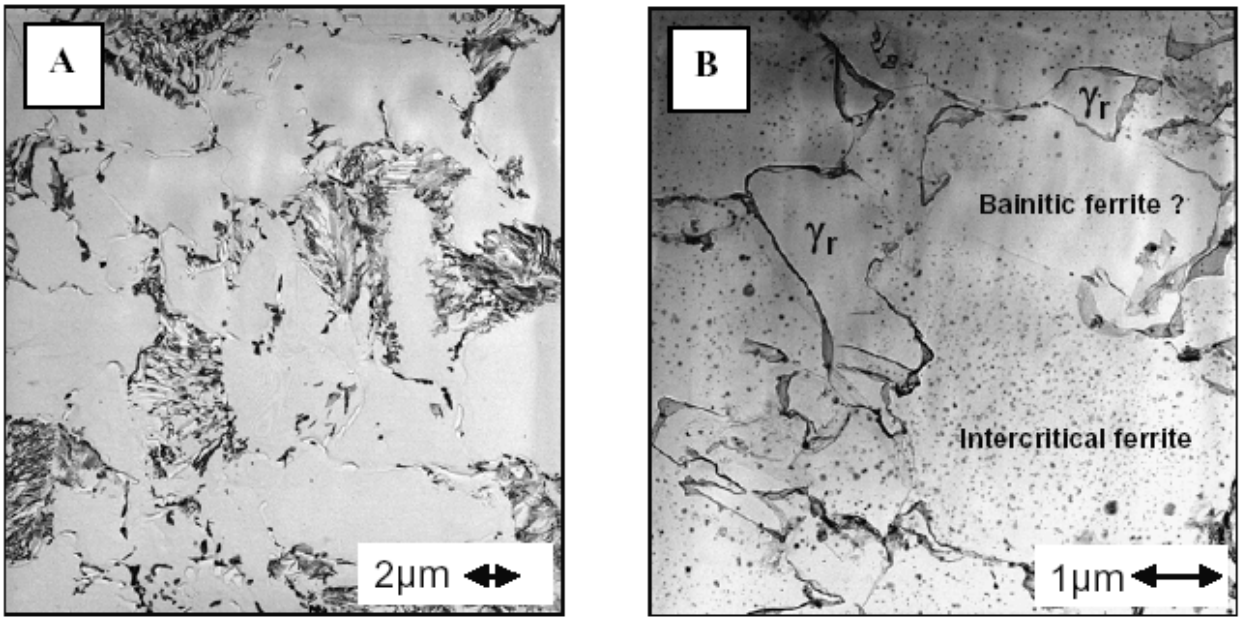

Fig.5 TEM alumina extraction replicas of (a) Heat B hot strip after coiling, (b)Heat B cold strip after annealing at 790℃ and overaging at 400℃

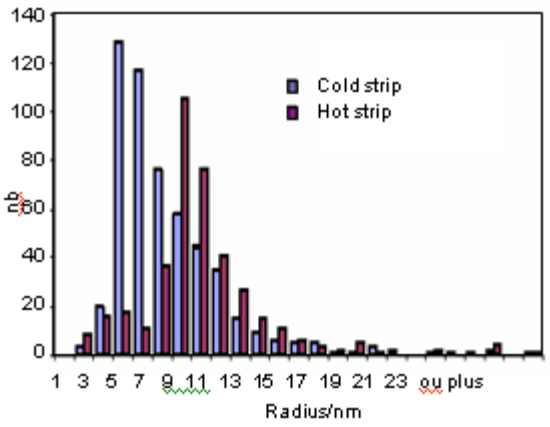

Fig.6 Precipitate size histograms from the hot coiled and cold rolled and annealed strip (Heat B)

2.8 Evolution of the precipitate composition

The precipitate composition as a function of precipitate size and position in the microstructure has been studied using PEELS and EDX. The V precipitates found in the hot strip ferrite all contain some fraction of Ti, even though this element was only present in residual quantities (0.003%wt.) in the original cast. In the cold strip, only a few precipitates containing Ti were found and these were mainly in the residual austenite and bainitic ferrite phases. The vast majority of precipitates present in the cold strip ferrite do not contain any Ti. We have compared the C/N ratios of the cold strip precipitates in ferrite and retained austenite as a function of precipitate size. Here we consider only particles which do not contain Ti, i.e. V(C,N). Figure 7 shows that there is a remarkable distinction between the two phases. V(C,N) precipitates in austenite show no particular correlation between their composition and size, and no large (>40 nm) diameter precipitates were found.

On the other hand, V(C,N) precipitates in ferrite show a very clear compositional evolution with precipitate size. The smaller precipitates (<30 nm) are similar to those found in the austenite with a C to N ratio which varies between 0.6 and 1.5. However, there exists in the ferrite a class of larger precipitates, which are more carbon rich (C / N ratio between 1.5 and 2.2). The carbon content appears to increase monotonically with precipitate size.

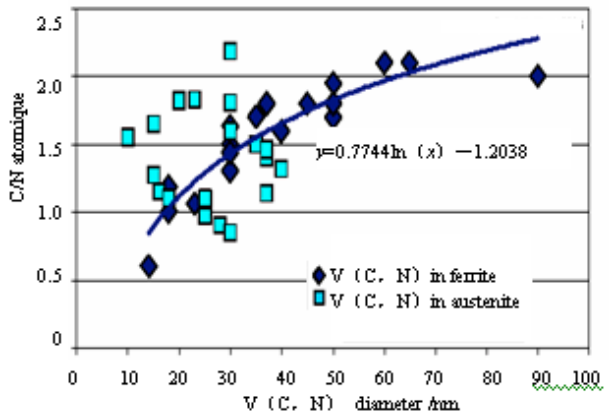

Fig.7 Comparison of the C/N atomic ratios in V(C,N) precipitates in the cold strip ferrite and in thecold strip austenite as a function of precipitate size (Heat B annealed at 790℃ and overaged at 400℃).

2.9 Quantitative study of the precipitation state during continuous annealing

The qualitative observations of the evolution of the precipitation state after continuous annealing have shown a high V(C,N) density in ferrite with very few precipitates in transformed austenite. In this section, we will firstly consider the evolution of the mean precipitation state and secondly the differences between the precipitation states in ferrite and in austenite.

2.9.1 Study of the mean precipitation state (in ferrite and in austenite)

Specimens were quenched at various points during the continuous annealing cycle as shown in Figure 8. The metal used was a fourth laboratory cast with a composition and thermomechanical treatment similar to Heat B but with a slightly higher V content. TEM replicas were examined to determine the precipitate size histograms and morphology. Selective chemical dissolution was used to determine the total weight fraction (wt. ppm) of Vanadium precipitated. The precipitated volume fraction was calculated assuming stoichiometric V(C,N). The table associated with Figure 8 shows the results. An average (Feret) radius for the precipitates was calculated from the size histogrammes.

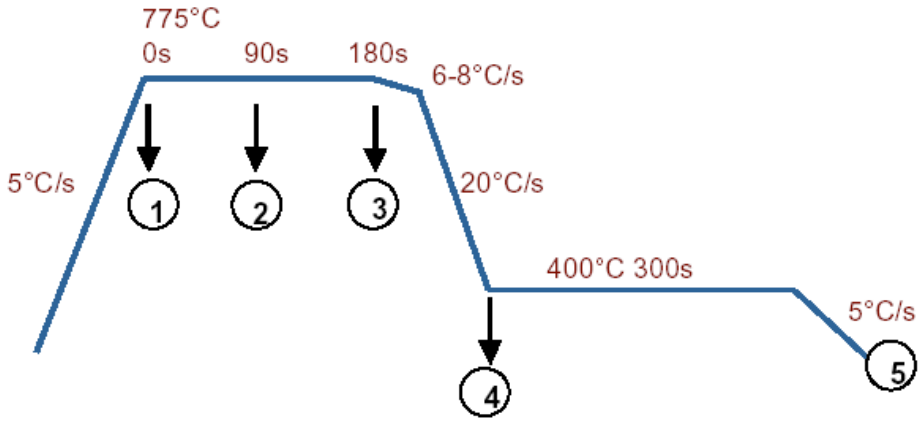

	1	2	3	4	5
Nb of particles	1679	714	1412	-	-
Feret radius (nm)	3.9	6.8	7.6	-	-
Elongation*	1.3	1.3	1.3	-	-
Precipitated V (wt ppm)	879	1049	1055	1105	1049
Volume fraction (ppm)	1408	1676	1690	1765	1676
Number density (μm^{-3})	5.67×10^{3}	1.27×10^{3}	9.20×10^{2}	-	-

Fig.8 Evolution of the mean precipitation state during CA composed of intercritical annealing at 775℃ and ageing at 400℃

The Feret radius (defined as the radius of a disk of area equivalent to the measured precipitate) ranges from 3.9 nm after heating to 775 °C and quenching at t=0 s to 7.6 nm after heating holding for 180 s at 775 °C. At the same time, the precipitated weight fraction of vanadium increases from 879ppm to a constant value of around 1050ppm, which we suppose to be the equilibrium value since it does not change between samples 2 and 5. Knowing the Feret radius and the total volume fraction of precipitate allows the number density N to be calculated. It can be seen from Figure 8 that the calculated mean density of precipitates N decreases during soaking. These results suggest therefore that the majority of nucleation and growth of V(C,N) precipitates is completed during the heating stage.

During isothermal annealing some coarsening of precipitates is observed, with an increase in the mean radius and decreasing number density at a constant precipitated fraction. The precipitation state was not quantified after the complete cycle (samples 4 and 5) because chemical analysis results show that there is no evolution of the precipitated weight fraction of vanadium during the final part of the CA cycle (cooling and overageing).

2.9.2 Differences between ferrite and transformed austenite

The mean radii of precipitates in austenite and in ferrite are compared in Table 4. Also shown are the relative fractions of austenite and ferrite at each holding time. This data was determined from dilatometry experiments. A most surprising result is that the mean precipitate radius in austenite and in ferrite is quite similar at all annealing times, with lower statistics in austenite because there are less precipitates2. This implies that during soaking the mean precipitate size in austenite increases at the same rate as that of precipitates in ferrite.

Table 4. Precipitation state in ferrite and in austenite after interrupted heat treatments.

	T (°C)	t(s) at T after heating at 5°C/s	% α	Nb of particles measured in ferrite	Feret radius (nm) (ferrite)	% γ	Nb of particles measured in austenite	Feret radius (nm) (austenite)
1	775	0	100	1679	3.9	0	-	-
2	775	90	37	583	6.7	63	131	7.4
3	775	180	36	1266	7.5	64	146	8.4

2.10 Qualitative description of the precipitation state after the complete CA cycle

The cold strip microstructure after the complete CA cycle is presented in Figure 9 for an intercritical temperature of 775°C (sample 5). At low magnifications one can easily detect residual austenite islands (micron sized grains with very few precipitates) embedded in a ferrite-bainite matrix (ferrite and bainite cannot be separated with this type of observation). Inside the ferrite/bainite matrix, a high density of V(C, N) precipitates is observed. Qualitatively, the mean precipitate sizes and densities do not appear to be different from those measured on samples quenched at the end of intercritical annealing. This is in agreement with the chemical analysis results which tell us that the precipitate d V fraction is unchanged. Some precipitates are present at the interface between ferrite and residual austenite islands, but no evidence of interface pinning either in the intercritical region or during the bainitic transformation was ever seen.

2. We tried to maintain the total area of austenite and the total area of ferrite used for precipitate quantification on the replicas constant at a given holding time. Note however that the total observed areas for different holding times were not the same.

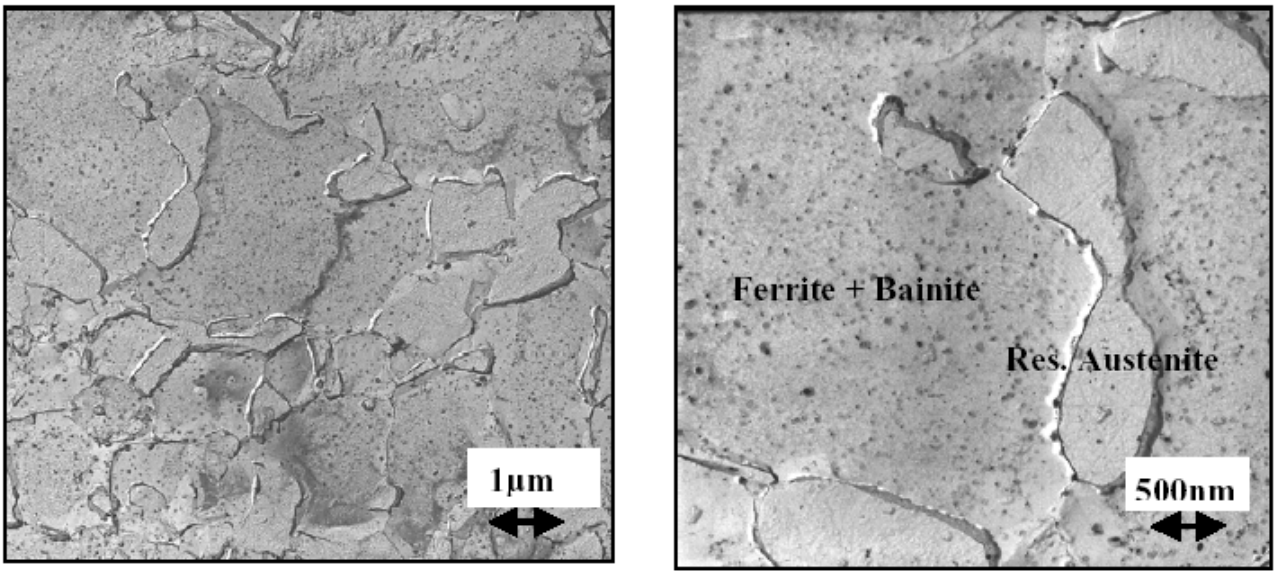

(775℃-180 s and 400℃-300s,sample quenched at point 5)

Fig. 9 TEM extraction replicas showing the precipitation state after continuous annealing.

2.11 Qualitative discussion of the complete precipitation sequence

Figure 4 showed that very little vanadium (～3%) was precipitated in heat B following quenching of the hot strip immediately after finish rolling at above 900℃. Thus, the reheating stage is sufficient to dissolve most of the large (Ti,V)N precipitates and smaller VN precipitates observed in the as-cast ingots[9]. After fast cooling and coiling at 540℃ the amount of precipitated vanadium increases to ～16%. PEELS and EDX analysis showed that essentially all of the precipitates detected at this stage were of the type (Ti,V)N with a size distribution between 10nm and 30nm [9] . PEELS measurements also showed that the carbon to nitrogen ratio in these particles was almost always less than 0.1. The sequence of vanadium precipitation in the hot strip can thus be represented as shown in Figure 10.

The most interesting point is the extremely strong influence of Ti and N on V precipitation in the hot band. Even for this grade, which contains <0.003%wt. Ti, every hot band precipitate observed contained some fraction of Ti. It seems highly likely that the presence of fine TiN precipitates formed at high temperatures acts as a nucleation site for V precipitation. If no Ti were present it is probable that the fraction of V precipitated after coiling could be still further reduced, thus facilitating the cold rolling process.

The cold strip precipitation processes occurring during final annealing are summarised in Figure 11. The sequence is complex due to the fact that precipitation takes place inside a two phase matrix which itself is in continuous evolution. Here we will describe the sequence of events and make a preliminary attempt to interpret some of the major experimental results. A proper detailed understanding requires the construction of a coupled kinetic phase transformation + precipitation model, which is a major long term objective.

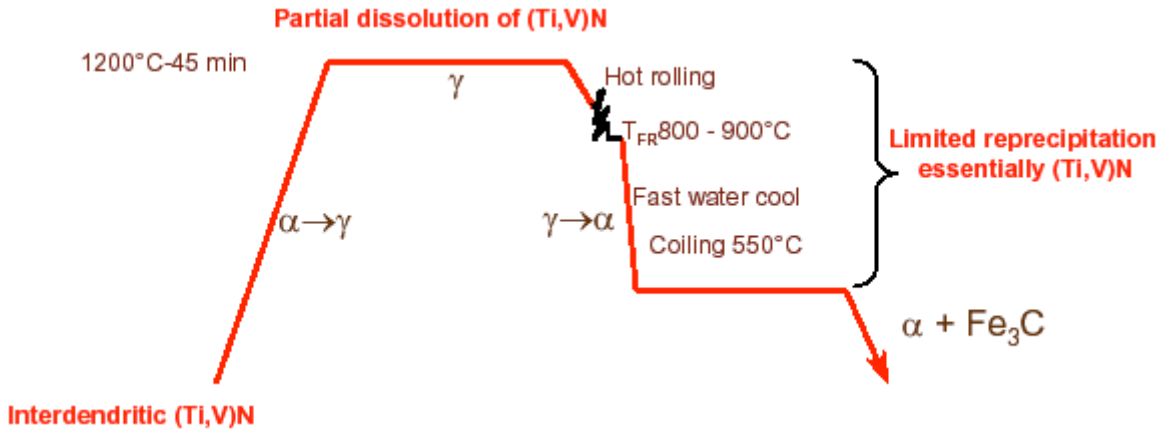

Fig.10 A qualitative description of V precipitation in the hot strip

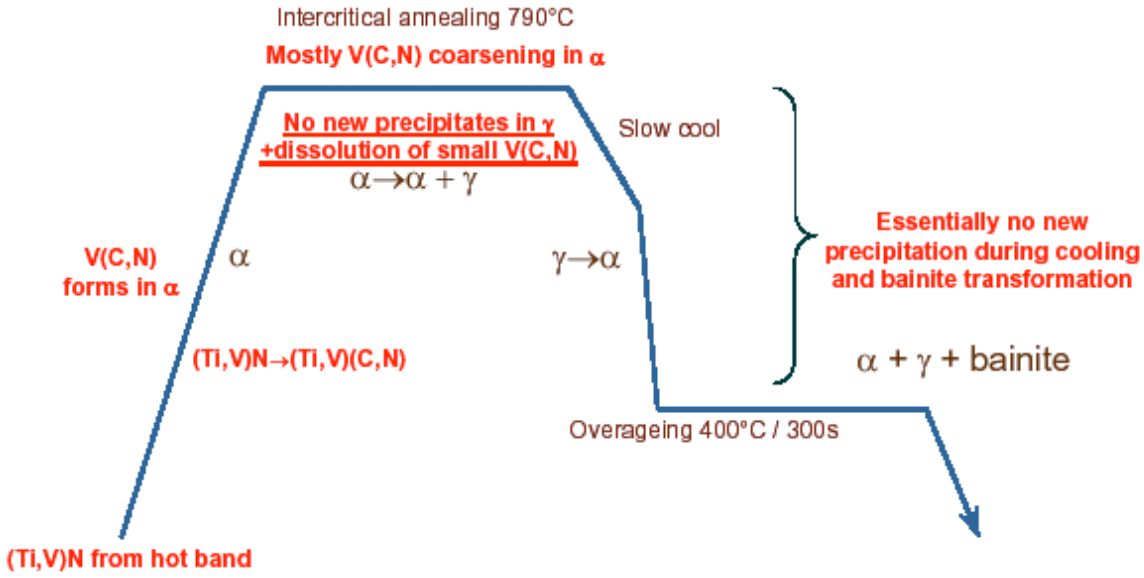

Fig.11 A qualitative description of V precipitation in the cold strip

We have shown that at the start of continuous annealing:

- The initial precipitation state is composed of some coarse (Ti,V)(C,N) precipitates and a small fraction of V(C,N) coming from the hot strip sequence. Assuming a coiling temperature of 540℃ less than 16% of the initial V is precipitated at this stage. Practically all of the residual Ti and about 50 ppm of N are precipitated (see Figure 4).
- During heating to the intercritical annealing temperature after cold rolling (when the sample is still 100% ferritic), we observe the intense nucleation and growth of new vanadium carbonitride precipitates.

At a heating rate of 5℃/s, the great majority of vanadium is already precipitated in ferrite before the start of the isothermal hold in the intercritical region. For example at 775℃, 879ppm (wt) of V is precipitated during the

heating stage compared with a total of ~1 050ppm (wt) V precipitated at the end of annealing. Thus the essential part of the V precipitation sequence takes place in ferrite during recrystallisation before the austenite transformation has begun.Precipitation during intercritical annealing at 775 ℃ :

• Once austenite starts to form during isothermal holding at 775℃ the evolution of V(C,N) precipitates in ferrite and in austenite is different. Under all conditions the number density of V(C,N) precipitates in intercritical ferrite is much higher than in austenite.

• For holding at 775℃, the equilibrium fraction of austenite (~63%) is attained at 90 s. During this time, the total fraction of precipitated V reaches the maximum value (~1050 ppm). This occurs by a combination of growth (the mean Feret radius increases from 3.9 to 6.8nm) and coarsening (the mean number density decreases from 5 670/μm^3 to 1270/μm^3) in ferrite. From 90 s to 180 s some further coarsening is observed, however the system is close to equilibrium and evolves slowly. The fact that the mean precipitate radius is similar at all times in both austenite and ferrite phases is difficult to explain and really requires a detailed modelling approach. One possible scenario is the following :

• From t=0s to t=90s V(C,N) precipitates continue to grow in untransformed ferrite. However during this time the volume fraction of ferrite decreases continuously from 100% to 37%. Precipitates growing in ferrite are initially N rich and gradually become carbon rich as their radius increases as seen in Figure 7.

• The solubility of V(C,N) in austenite is much higher than that in ferrite, so that in the newly nucleated austenite grains the critical radius for V(C,N) stability is larger. V(C,N) particles inherited from the prior ferrite whose radius is smaller than the new critical radius will thus be unstable and will dissolve. It is also likely that the inherited precipitated fraction of V(C,N) in new austenite is higher than the equilibrium value, thus stable precipitates with larger radii will not grow. This is in agreement with EELS data of Figure 7 which showed no dependence of V(C,N) composition on precipitate size in austenite. Thus the number density of V(C,N) in austenite decreases and heir mean radius increases due to dissolution (and not coarsening).

• From t=0s to t=90s, the rate of precipitate growth in ferrite must be slightly higher than the rate of dissolution in austenite so that the overall weight fraction of precipitated vanadium increases and the mean radius increases (due to growth and coarsening in ferrite and dissolution in austenite) at the same rate in both phases.

• From 90 s to 180 s the system approaches equilibrium and the precipitate radii do not greatly change.

No further evolution of the precipitation state is seen during cooling and bainitic holding.

3 Conclusions

We are now in a position to explain qualitatively why vanadium TRIP steels exhibit a decrease in UTS with increasing intercritical annealing temperature, whereas for nonmicroalloyed TRIP grades this is not the case (figure 3). As the intercritical annealing temperature is increased, two things happen :

• The fraction of austenite formed will increase and thus the total amount of V precipitated will decrease.

• The rate of coarsening of V(C,N) in ferrite will increase.

Both of these factors combine to reduce the effectiveness of precipitation strengthening. In order to optimise the V precipitation effect it is obvious that the intercritical annealing temperature should be kept as low as possible and that the annealing time should be as short as possible. Of course, the annealing parameters must always be kept compatible with the requirement to produce a microstructure with the correct phase fractions to mainain a good TRIP effect, so that the final choice must always be a compromise. Concerning potential industrial applications it is clear that the most critical process

parameters controlling the final mechanical properties of microalloyed TRIP steels are the intercritical annealing temperature and the line speed.

4 Acknowledgements

This work was part financed by an ECSC award (project 7210-PA-295). The authors would also like to thank Vanitec PLC and especially P. S. Mitchell for the invaluable support and encouragement shown.

References :

[1] Horvath C D and Fekete J R,. Opportunities and Challenges for Increased Usage of Advanced High Strength Steels in Automotive Applications, Proc. Int. Conf. on Advanced High Strength Sheet Steels for Automotive Applications (2004). Winter Park, Colorado: pub AIST, pp3-10.

[2] Bai D O, et al., Stability of Retained Austenite in a Nb Microalloyed Mn-Si TRIP Steel. Mat. Sci. Forum 284-286 (1998), pp 253-260.

[3] Wang J and Van der Zwaag S., Stabilization Mechanisms of Retained Austenite in Transformation-induced Plasticity Steel. Metallurgical and Materials Transactions A, (2001), 32A, pp 1527-1539.

[4] De Cooman B C., Structure-properties Telationship in TRIP Steels Cntaining Carbide-free Bainite. Current Opinion in Solid State and Mat. Sci. 8 (2004), pp285-303.

[5] Hanzaki A Z, t al., The Retained Austenite Characteristics in a Thermomechanically Processed Nb Bearing TRIP Steel. Proc. Symp. High-Strength Steels for Automotive (1994), p53.

[6] Bleck W, et al., Effect of Niobium on the Mechanical Properties of TRIP Steels.Mat. Sci. Forum 284-286 (1998), p327.

[7] Pereloma E V, et al., Transformation Behaviour in Thermomechanically Processed C-Mn-Si TRIP Steels with and without Nb. Mat. Sci Eng. A273-275 (1999), pp448-452.

[8] Lian S and Hua L., Effect of Retention and Mechanical Stability of Retained Austenite on Tensile Properties in Low Carbon - Low Alloy Triphase Steel. Mat. Sci. Tech. 11 (1995), pp499-507.

[9] Scott C, et al., Microalloying with Vanadium in TRIP Steels. in proc. Int. Conf. on Advanced High Strength Sheet Steels for Automotive Applications. (2004). Winter Park, Colorado: AIST, pp181-193.

[10] Eberle K, et al., New Thermomechanical Strategies for the Production of High Strength Low Alloyed Multiphase Steel Showing a Transformation Induced Plasticity (TRIP) Effect. Steel Res. 70 No.6, (1999), p233.

[11] Gladman T., The Physical Metallurgy of Microalloyed Steels. The Institute of Materials (1997).

[12] Lagneborg R, et al., The Role of Vanadium in Microalloyed Steels. Scandinavian Journal of Metallurgy 28 (1999).

[13] Balliger N K and Honeycombe R W K., The Effect of Nitrogen on Precipitation and Transformation Kinetics in Vanadium Steel. Metallurgical Transactions A, (1980). 11A: pp. 421-429.

[14] Scott C, et al., ECSC Steel RTD Programme project 7210-PA-295: New Metallurgy for Microalloyed TRIP Steels. Technical report n°5, (2003).

[15] Lehmann J., Nouvelle version de CEQSCI pour la déscription des séquences de précipitation lors de la solidification du métal: oxydes, sulfures, nitrures, carbures. Arcelor internal report PCMO/PC 00 N25 (2000).

[16] Perlade A, et al., A Physically Based Model for TRIP-Aided Carbon Steels Behaviour. Mat.Sci. & Eng. A356 (2003), pp145-152.

[17] Scott C, et al., Quantitative Analysis of Complex Carbo-Nitride Precipitates in Steels. Scripta Mat. 47 (2002), p.845.

[18] Scott C, and Drillet, J., Quantitative Analysis of Local Carbon Concentrations in TRIP Steels. Steel Res 73, 6+7, (2002) pp 97-102.

[19] P.Maugis, M. Gouné., A computer model of carbonitride precipitation in steel.Proc. of IAC3 conference, Estoril, July (2002).